

Radio Local Area Network (RLAN) and C-Band Weather Radar Interference Studies

Paul Joe¹, John Scott¹, John Sydor², Andre Brandão² and Abbas Yongacoglu³

¹Meteorological Service of Canada, 4905 Dufferin St., Downsview, Ontario, Canada, M3H 5T4

²Communications Research Centre, 3701 Carling Avenue, Ottawa, Ontario, Canada K2H 8S2

³University of Ottawa, Ottawa, Ontario, Canada

1. Introduction

There is a growing concern about the effect that wireless internet devices operating at 5 GHz will have on the operation of weather radars. At the World Radio-communication Conference 2003 (WRC-2003), the decision was made provide a primary allocation to the mobile service for the implementation of wireless access systems (WAS), including radio local area networks (RLAN), in the band 5470-5725 MHz (ITU-R 229, 2003). The operation of RLANs in this band is permitted as long as they do not cause interference to licensed services such as Radiolocation, which operate in the 5600-5650 MHz sub-band (C-Band). The RLAN bands consist of 10 channels, each with 18 MHz bandwidths. Typical C-Band weather radars operate with 0.5 or 1 MHz bandwidths. There are 2 RLAN carrier bands that are very near or within the weather radar C-Band.

Radar and WAS technologies are expected to co-exist in the same environment through a frequency abandonment protocol by the RLANs. The RLANs are required to implement a Dynamic Frequency Selection (DFS) system in which radio-frequencies are monitored and the RLAN selects frequencies that are not used. Before using a channel, the RLAN must check for the presence radar signals for a 60-second period. Once the RLAN is using a channel, it must continue to monitor for the presence of radar signals. If these signals are detected, RLANs must vacate the channel for a 30-minute period. In addition, before re-using the channel, the RLAN must continuously monitor the channel for a 10-minute period. The RLANs can also choose to notch out the sub-band 5600-5650 (channel exclusion). These latter requirements were put forward by Canada to protect its weather radars and were adopted by the WRC-03.

The 10 minute monitoring closely matches the scan cycle time of a weather radar but it is a compromise since some radar systems scan with longer cycle times. Using this strategy, the

RLANs would theoretically not use the weather radar frequencies in their presence.

There has been very little experimental work to test and verify the efficacy of the DFS systems. The proposals were based on many assumptions and simulations (ITU-R 8A/103-E 8B/65-E, 2004).

This note documents experiments on: (i) the nature of the RLAN interference that would be seen by the weather radar, (ii) the detection thresholds of the DFS/RLAN's to see the weather radar signal (Brandão et al, 2005), (iii) simulating a network of RLANs in a rural-urban environment and estimate the effect on weather radars.

2. The Experiments

There were two sets of experiments. The objective of the first experiment was to test, calibrate and verify the response of the radar to RLAN signals by directly injection ahead of the receiver (see Fig. 1). The objective of the second set of experiments was to test the effect of the inclusion of the antenna and propagation environment as well as to test the detection capabilities of a DFS. Finally, these data were used in a simulation of a network of operating RLAN's in an urban environment.

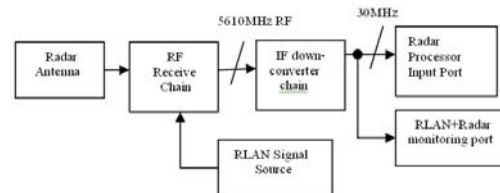


Figure 1: Block diagram of a radar showing the location of where the RLAN signal was inserted for the first set of experiments. This is similar to a typical receiver calibration procedure

For the first set of experiments, RLAN signal power levels and modulations were varied and weather radar spectrum and power measurements were made using Sigmet's

ASCOPE recording capability. Reflectivity parameters were recorded and converted to power measurements using the radar equation. Power measurements were referenced at the input of the signal processor.

This is was similar in the second set of experiments except the RLAN signals were transmitted using an antenna on a mast (7 or 15 m in height). Two locations at different ranges (0.5 and 10.6 km) where used. In addition, the radar operated in a staring mode whilst DFS receiver measurements were made to test its sensitivity to radar signals.

3. The RLAN Signal

RLAN signals are bursty in nature. During a burst, packets of information can be transmitted at various modulations or pulse rates in 10 carrier channels within the newly opened 5470-5725 MHz. This is compared to the weather radar C Band frequencies of 5600-5650 MHz. The RLANs already used 5250-5350MHz and 5725-5825MHz in Canada and elsewhere.

The RLAN modulation schemes are expected to use the full 18 MHz bandwidth of each channel. The weather radar, with its typical 0.5 or 1 MHz bandwidth for a 2 μ s or 1 μ s pulse, respectively, will see these RLAN signals as additive white noise and not at a particular Doppler frequency which would be the case if the RLAN bandwidths were smaller than about 1 MHz.

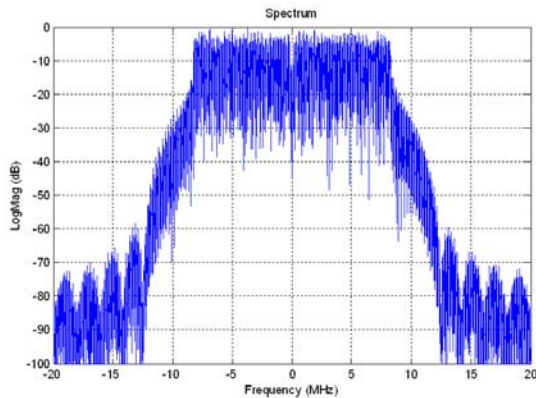


Figure 2: The frequency spectrum of the simulated RLAN signal.

The source for RLAN signals was an Agilent 4438C ESG vector signal generator capable of generating IEEE 802.11a packets of adjustable payload and length. For this experiment, the payload consisted of a pseudo-random packet resulting in, with the addition of the IEEE

802.11a header, a 750 microsecond long packet. Unless otherwise stated the packet inter-arrival time was set to zero for these experiments to ensure overlap of radar pulses and RLAN packets. In actual operation, the inter-arrival time of RLAN packets from a single source is typically orders of magnitude longer than their length.



Figure 3: Experimental setup for the external tests, showing the 16 m (maximum) extendable mast (left) with the DFS detector and the RLAN antenna (upper right) and the RLAN equipment located in the van (lower right).

The centre frequency of the RLAN radio emissions, the modulation format, and the mean signal power were adjustable. For this experiment, unless otherwise specified, the RLAN signal was modulated at an 18 Mb/s rate using QPSK/OFDM¹ modulation, as specified by the IEEE 802.11a standard. The center frequency of the RLAN signal overlapped the radar signal at 5610 MHz. The RLAN spectrum is shown in Figure 2. The spectrum shows a flat

¹ QPSK/OFDM means Quadrature Phase Shift Keying/Orthogonal Frequency Division Multiplexing. It is beyond the scope of this note to describe this in detail but, suffice it to say, that this simulates a RLAN signal.

spectrum with 30-40dB variations in power over 18 MHz frequency range with the first side lobe at about 60 dB down.

The RLAN packet generator had the flexibility of being connected directly to the CWSR98 5 GHz receiver chain for the indoor tests, as shown in Figure 1. For outdoor tests the generator was connected to a 10 watt Class A linear power amplifier, then via a calibrated cable to a 12 dBIC circularly polarized antenna that was mounted on an adjustable mast (Fig. 3). Using this technique a signal of 38 dBm EIRP² was capable of being generated. Typically an IEEE 802.11a RLAN does not radiate more than 23 dBm; by regulation and RLAN device is not allowed to radiate more than 30 dBm.

4. The Radar

Franktown radar (call letters XFT, 45.04446°, -76.06423°), an operational C-Band radar of the Meteorological Service of Canada, was used for the experiments (Lapczak et al, 1999; Joe and Lapczak, 2002). The radar characteristics are shown in Table 1.

The radar is located in relatively flat, forested terrain. A small urban community, Carleton Place, is located about 10 km away where the external experiments were conducted. Two pulse widths are available (0.8 and 2.0 μs) corresponding to bandwidths of 1.25 and 0.5 MHz. Note the 0.65° beamwidth, which for all other radar characteristics being equal, results in higher gain and hence greater sensitivity than the more common 1° beamwidth radars.

5. The Dynamic Frequency Selector

A commercial DFS detector was not available at the time of the experiment. A typical detector was constructed using off-the-shelf detection diodes, RF amplifiers, and bandpass filters. The detector was attached by a calibrated cable (-8 dB loss) to an omni directional antenna having a nominal -1 dBi gain. Fig. 4 shows the response curve of the detector to pulsed power (detector power readings should have 10 dB added to them to scale them to the level seen at an output of 0 dBi antenna, as stipulated by the ITU requirements). The response of the detector to a typical 0.8 microsecond wide radar pulse is shown in Fig. 5. The response time of the

² EIRP means Effective Isotropic Radiated Power.

detector is in the order of 50 nanoseconds. For the outdoor experiments, the DFS detector antenna was mounted on the adjustable mast in proximity to the RLAN antenna (see Fig. 3).

Parameter	Units	
Diameter	m	6.1
Beamwidth	°	0.65
Gain	dB	47.5
Polarization		H
Az rate	°/s	3-36
Frequency	GHz	5.625
Wavelength	cm	5.32
Peak Power	kW	250
Pulse Length	μs	0.8, 2
PRF	Hz	1190, 250
Bandwidth	MHz	1.25, 0.5
MDS at 1km	dBZ	-31.8125, -38.3750
Noise (meas)	dBm	-103, -108
A/D	bits	12
No. of Range Gates		256
Gate Spacing	M	50, 125

Table 1: Typical characteristics of a 0.65° beam width MSC radar, used for the study.

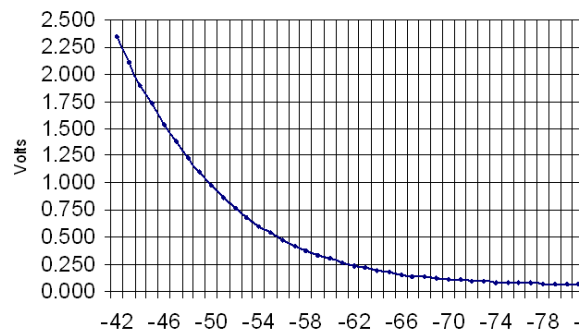


Figure 4: Response of the DFS to pulse power detected.

6. Response of the Radar to RLAN Signals

RLAN signals were directly injected into the receive port of the weather radar as well as from an external source to verify the additive noise nature of the interference on the weather radar signal. The tests are described in Table 2. Fig. 6 shows the results of these threshold and performance tests. All the tests were done with the 0.8 μs pulsewidth which corresponds to a 1.13 MHz bandwidth, as it represents the worse case scenario. The results are described in units of power [in dBm] and are referenced to the input of the signal processor (and not to the front end of the antenna). The RLAN signal

levels are also referenced to the input of the signal processor taking into consideration all the path losses. The results show that the weather radar is able to detect the RLAN signal corresponding to the minimum signal power. While this may seem intuitive, *a priori*, it was not necessarily true considering the various sophisticated levels of filtering, down converting and processing that occurs with the received signal (Joe et al, 1998).

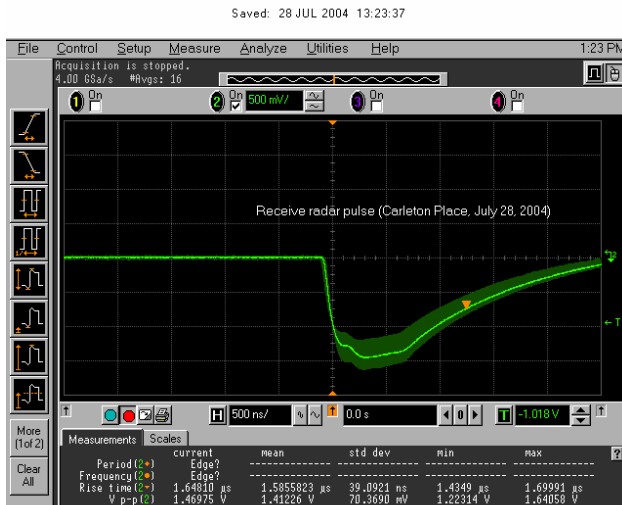


Figure 5: Response time of the DFS detector for a radar-DFS separation of 10.6km. Detector reaction time on the leading edge is about 50 ns.

The linear response of the radar confirms the additive nature of the RLAN signal. The slight change in the noise level of test 6 is due to a change in elevation angle. The fall off of the results for test 7 is indicative of a power supply failure in the RLAN which prematurely ended the testing.

What is interesting is that the radar was able to pick up the RLAN signal from the 500m site even when the antenna was not directly pointed at the RLAN source. For test 3, the radar was able to detect the RLAN through the side lobes of the antenna either directly or from multi-path reflections. For test 4, the radar was able to detect the RLAN from backscatter from the vegetation in the surrounding environs.

The effect of duty cycle of the RLAN was evaluated by various the bit rate of the RLAN signal from 18 MBPS to 54 MBPS and by varying the inter-arrival time (0 to 10,000 μ s) of

fixed length packets (750 μ s) The average power of the packet was fixed at -20 dBm.

Label	Description
1 Day 1 Series A Injection Test	RLAN signals are directly injected into the front of the downconverter. The transmitter is off.
2 Day 2 Series A – 500 m site	RLAN signals are transmitted from a ~15m mast positioned 500m from the antenna in a rural environment. Signal is peaked.
3 Day 2 Series B – Off axis test	Repeat of previous experiment with the antenna pointed 60° off axis in azimuth and elevation.
4 Day 2 Series C Backscatter test	Repeat of previous experiment with the antenna pointed in the opposite direction to the mast.
5 Day 3 Series A 10 km Site	Repeat of Test 2 with a 15m mast, located in a small rural community with intervening rural environment, 10km away at Carleton Place, Ontario.
6 Day 3 Half Mast	Repeat of the previous test, with the mast lowered to 7 m.
7 Day 3 Injection Test Transmitter On	Repeat of Test 1, with the transmitter on.

Table 2: Description of the RLAN tests with continuous RLAN signals.

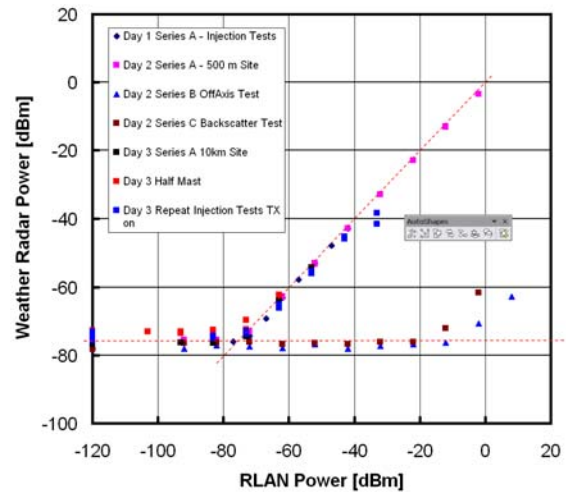


Figure 6: Power injection measurements. See Table 2 for a description of the tests. The practical background noise observed in the experiment is about -78dBm whereas the nominal SNR of the radar is around -80dBm. Therefore, backscatter at 500m is not visible by the radar when the interference is below the nominal SNR of the active radar.

The results (fig. 7) show that the radar response is directly proportional to the duty cycle reinforcing the conclusion that RLANs are seen as additive noise.

The frequency of the RLAN carrier frequency was offset by 2 KHz from 5610MHz but this did not produce a noticeable effect. This was not unexpected as the RLAN signal covers an 18MHz bandwidth. The frequency was then shifted by 15 and 65 MHz (to the next carrier frequency) and the RLAN signal was not detected by the radar (Fig. 8).

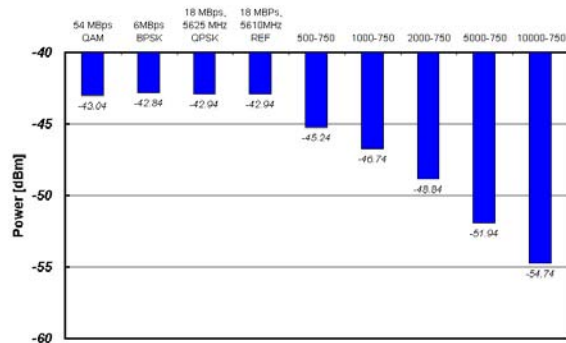


Figure 7: Variation in modulation, bit rate (left four experiments) and inter-arrival time of the RLAN packets (right five experiments). Little variation is observed due to modulation (QAM, BPSK nor QPSK)³. Inter-arrival time affects the results in a proportional fashion, the first number indicates the inter-arrival time and the second number the packet length...



Figure 8: Frequency off-set variation. Variations of the order of a KHz have the same effect whereas shifts of 15 and 65 MHz in the RLAN carrier frequency are not detectable by the weather radar.

Fig. 9 through 13 show PPI, RHI and Xsect (arbitrary cross-section displays) of the RLAN signal when the source was located at 0.5km

³ QAM means Quadrature Amplified Modulation; BPSK means Bi-phase Shift Keying and QPSK means Quadrature Phase Shift Keying. These are various RLAN signal modulations.

and 10.6 km from the radar. The results from the 0.5 km site may not be a realistic scenario since it is presumed that a RLAN would not operate effectively so close to weather radar. However, it is educational to reveal the nature of the interference signature. In Fig. 9, the radar was operated in its normal 24 elevation scan mode with the lowest elevation angle being 0.3°. The RLAN signal can clearly be seen in ~30° sector just south of the radar. The signal is seen not only in the main lobe but in the side lobes of the radar.

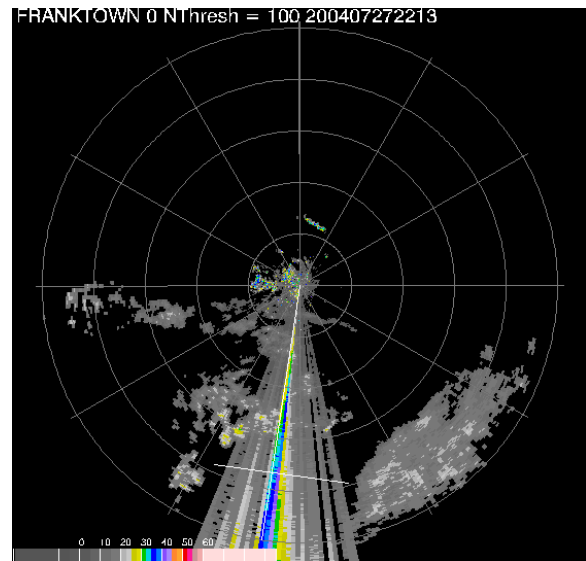


Figure 9: A PPI display at 0.3° elevation angle of a RLAN at a distance of 500m from the antenna. The RLAN signal shows as uncorrelated noise. Doppler velocities (not shown) had a white noise spectrum. The white lines indicate cross-sections shown in the next two figures.

A cross-section in the cross-beam direction shows the azimuthal and elevational behavior of the signal (Fig. 10). The signal is sufficiently strong to be detected at an echo power equivalent to a 40 dBZ echo at 200km revealing the antenna pattern of the radar.

Fig. 11 shows a RHI display through the strongest part of the echo and again shows what appears to be a map of the antenna beam pattern in the vertical plane.

Fig. 12 shows a PPI display of the RLAN signal when the source is 10.6 km from the radar. The path loss is such that the signal is only seen in the main lobe of the antenna both in azimuth and elevation (not shown). This is more typical of what would be expected.

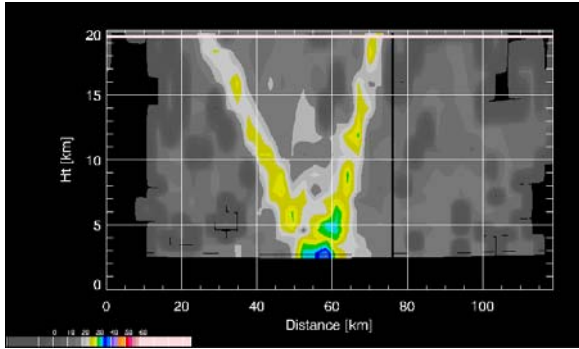


Figure 10: A cross-section made in the cross-beam direction (see previous figure) showing the azimuthal and vertical structure of the RLAN signal. The RLAN is located at 500 m from the radar and so it is seen not only in the main lobe but also the side lobes of the antenna

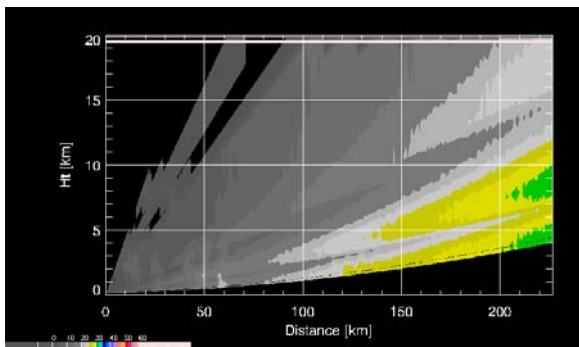


Figure 11: A RHI reflectivity section taken in the beam direction, showing the vertical interference structure of a nearby RLAN signal.

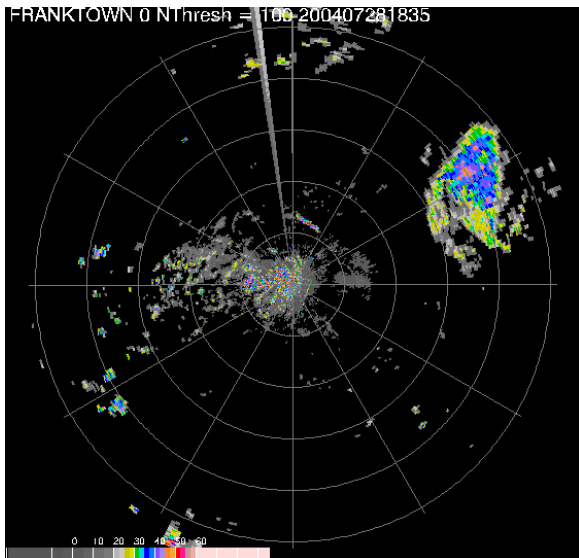


Figure 12: A low level PPI scan (0.3°) for the same RLAN source as in the previous figures but located 10.6 km from the radar. The signal was only seen in two azimuths and two elevations scans.

The last example is a PPI display for the case of the RLAN source located at 0.5km away (Fig. 13). In this example, the elevation angle is 4.14° . The strong RLAN signal can be seen in the side lobes located approximately 110° from the main lobe. Again, this is an educational example and probably not realistic.

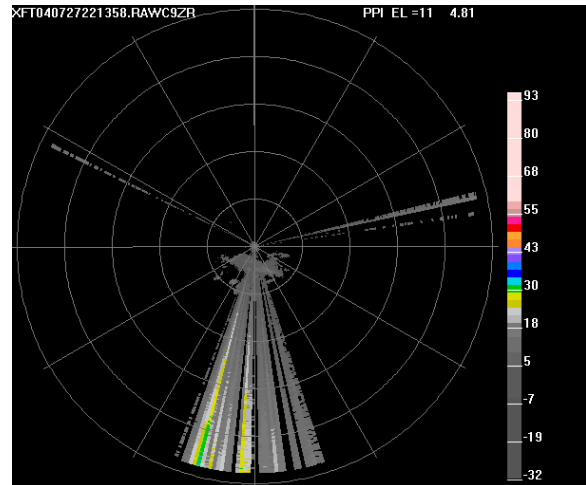


Figure 13: An elevated PPI display at 4.14° elevation angle of a nearby RLAN source. The RLAN can be seen in the side lobes located at about 110° from the main lobe.

7. Response of the DFS to Radar Signals

Critical to the co-existence of weather radar with RLANs is the ability of the DFS to detect radar signals. Fig. 5 shows that a DFS located 10.6 km from the radar in a mainly rural environment can detect the radar with a power level of about -36 dBm and -55 dBm, for a 15 m and a 7 m mast height, respectively. The threshold design requirement for detection is -64 dBm. For the 15 and 7 m mast heights, the Path Loss Exponent was experimentally determined to be 2.8 and 3.2 and correspond to 160 and 176 dB signal attenuation over 10.6 km.

A RLAN with a 30 dBm (maximum design limit) would be detected at -51 and -70 dBm or about 19dBm above and at the weather radar detection limit, respectively. In the latter scenario, the RLAN sees the radar but the radar does not see the RLAN. In the former situation, each sees the other. With high path loss environments, the detection of the weather radar signal can vary significantly (20-25 dB) and complicates the analysis.

Even the power from the side lobe could be detected by the DFS (at range 500m, Fig. 14) but this would require sophisticated signal processing in the DFS to detect (compare to Fig. 5).

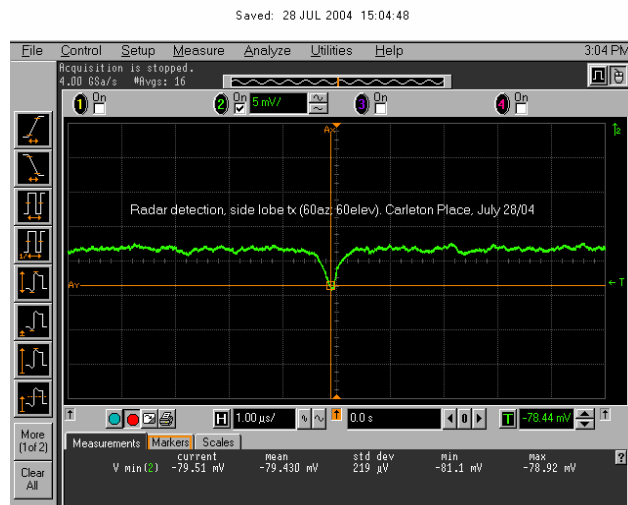


Figure 14: DFS detection of an antenna pointed 60o away in azimuth and in elevation away from the DFS.

8. RLAN Network Simulation

The experiments provide information regarding the performance of radar and a RLAN with a DFS. Given this information, the performance of a network of RLANs (including Access Points and Stations) can be assessed. There are many outstanding questions: (i) what happens when there are many RLAN systems, (ii) how channels are selected, (iii) when and how quickly channels are vacated, (iv) what happens when RLANs arrive and depart the network, (v) will RLAN systems be built with full 10 channel capability, (vi) channel move algorithm using the 30 minute rule and the 30 minute plus 10 minute monitoring rule in the presence of radar signals and (vii) will multiple RLANs each operating below radar threshold levels, combine additively to create a radar detectable signal and many other questions. It is beyond the scope of this brief report to respond to all these questions. A brief example will be given to illustrate the nature of the analysis but will be summarized in the conclusions.

A statistical simulation was performed assuming parameters of the King City radar and the city of Toronto and environs. The King City radar is located on the Oak Ridges Moraine (43.96389°, -79.57147°), 30-40km north of the major urban

city of Toronto. Between the city center and the radar, there is a sprawling suburban and rural environment. This environment was used to assess various scenarios and represents a worse case scenario in Canada. RLAN's were randomly distributed in 3 concentric rings (4km-urban, 12km-suburban and 25km-rural) around the city center according to the ITU-R M.1652 model. On average, there are 1652, 826 and 725 active systems in the three zones (Fig. 16) and are distributed with respect to height, building type and building location, among other considerations.

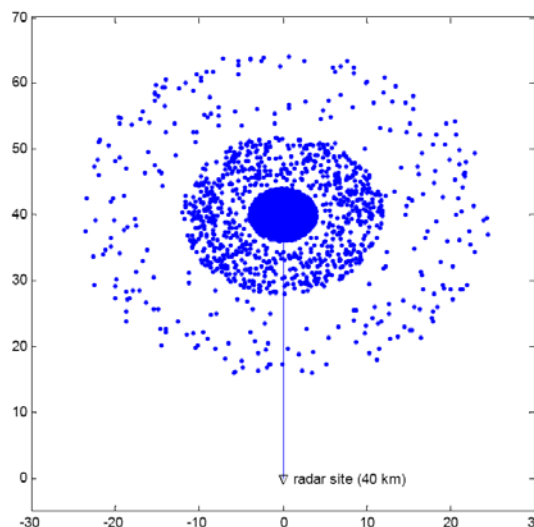


Figure 15: Assumed distribution of RLAN for simulation studies.

Given this scenario, only those RLAN's that are above the radar horizon and who receive radar pulses at power levels below -62 dBm, the DFS detection threshold, can be statistically estimated. An example of a single realization is show in Fig. 17. This shows that without DFS protection, many RLANs have the potential to interfere with the weather radar.

From the survivors, the maximum RLAN signal at the radar can be computed. The ITU distribution of RLAN characteristics is used (they may have different power outputs). Results assuming a 25m tower, 250kW radar are computed for two different antenna gains and as a function of DFS threshold are presented in Fig. 18. The results indicate the output of the surviving RLANs are below the minimum detection limit of the weather radar and so the -62 dBm DFS detection limit is sufficient.

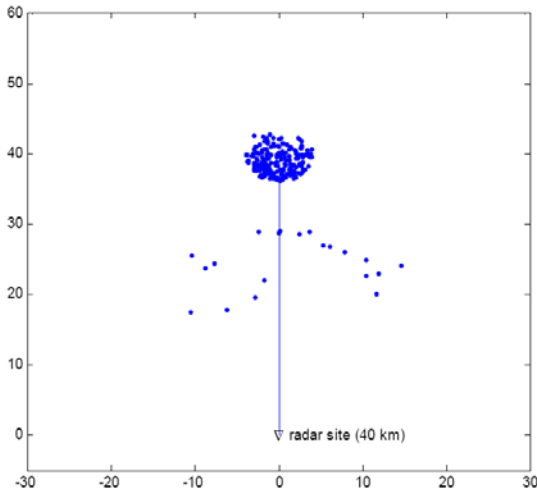


Figure 16: Surviving RLAN systems taking into consideration the radar horizon and given a DFS threshold of -62 dBm. This assumes the radar site locations of King City radar.

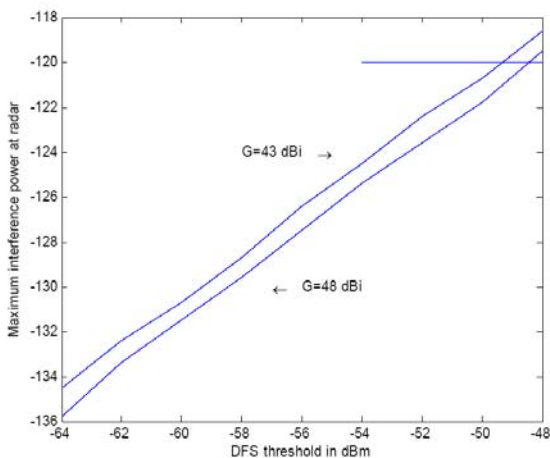


Figure 17: An estimate of the maximum interference at the radar as a function of the DFS threshold for two different antenna gains (equivalent to a 0.65° and 1.0° beam). The horizontal line indicates the radar sensitivity of -120dBm.

9. Summary and Conclusions

Experiments were conducted for the first time (i) to measure the performance of weather radar to various RLAN signals, (ii) to measure the performance of a prototype Dynamic Frequency Selector and (iii) to simulate a network of RLANs in a rural-urban environment.

RLAN signals appear as additive white noise and can be detected at the minimum detection limit of the weather radar. Since, the RLAN signal adds to the noise of the radar and so degrades the ability of the weather radar to

detect weak targets. While there is no phase degradation for strong targets, the additional noise affects the measurement of the velocity for weak targets. However, there is no phase shifting of the weather radar echo. The degradation of polarization signals is unknown and this will depend on the design and implementation of the RLAN transmitters (will they be horizontally, vertically, circularly or other polarized). There were no RLAN/DFS commercial systems at the time of the experiments.

A DFS threshold level of -62 dBm appears sufficient to protect the radar in the presence of radar pulses. When the radar is not protected (for example, while it is scanning at higher elevations) by radar pulse triggered DFS detectors, then the system is vulnerable to interference. Even a single interferer can exceed the threshold, and in some cases by about 50 to 60 dB. Most high level interferers may be de-activated by radar pulses received before the peak of the beam illuminates the interferer. This is more applicable to slowly scanning radars and will depend on the channel evacuation algorithms. So, access points should have delayed access to the system. This means that before using the weather radar channel, they should monitor for ten minutes and ensure that radar pulses are not present in the channel regardless of whether the systems have or not have channel move capabilities. From the simulations, surviving RLANs are far from the radar, so they should not pose a threat to the radar.

Radars with broader beams, that see more RLANs in their main lobe, will result in more residual interference. Radars with lower powers would not be detected so easily by the DFS and therefore this would result in larger number of surviving RLANs and therefore more residual interference given the same minimum detection sensitivity. Radars with higher antenna heights will be exposed to more interferers because of their larger radio horizon.

An open question remains as to the ability of the RLANs to detect the radar early enough to turn off in time to prevent interference. At this time, there are no commercial RLAN's and an RLAN signal simulator was used for the tests.

Not discussed in this report are spurious signals from out of band RLAN channels. With the upgrade of the King City radar to polarization

capability, new interference sources were noticed which were the result of out of band signals that were not filtered by the receiver. Additional filtering was required to eliminate the effect of these signals.

Algorithms for measuring noise and to extract echoes in weather radar signal processing will have additional challenges to adjust to dynamically changing noise environments created by RLANs and other wireless technologies in the future. With increasing wireless technologies, there are constant new threats to radio-frequencies used by the meteorological community and diligence is required. New threats include the ultra-wideband technologies.

10. Acknowledgements

This study was supported by Industry Canada. The weather radar community in Canada greatly appreciates the efforts by Industry Canada for their efforts in the protection of weather radar radio-frequencies. We also acknowledge the support Wayne Brett and Derek Hung who assisted in the measurements, the National Radar Program and the Ontario Weather Centre for allowing the use of the operational radar for these tests.

11. References

Brandão, André L. , John Sydor, Wayne Brett, John Scott, Paul Joe, Derek Hung, 5GHz RLAN Interference on Active Meteorological Radars, IEEE VTC2005-Spring, Stockholm, Sweden, May 30 – June 1, 2005

ITU-R Radio Communication Study Groups, documents 8A/103-E and 8B/65-E, August 30, 2004, "Studies on the effect of wireless access systems including RLANs on terrestrial meteorological radars operating in the band 5600-5650 MHz", International Telecommunication Union (ITU), Geneva, Switzerland.

ITU-R Resolution 229 [COM5/16], "Use of the bands 5150-5250MHz, 5250-5350MHz and 5470-5725MHz by the mobile service for the implementation of wireless access systems including radio local area networks", The World Radio-communication Conference (WRC-03), Geneva, 2003.

ITU-R Recommendations, Series M, document M.1652, June 2003, "Dynamic frequency selection (DFS) in wireless access systems including radio local area networks for the purpose of protecting the radio-determination service in the 5 GHz band", International Telecommunication Union (ITU), Geneva, Switzerland.

Joe, P., D. Hudak, C. Crozier, J. Scott, R. Passarelli Jr., A. Siggia, 1998: Signal Processing and Digital IF on the Canadian Doppler Radar Network, Advanced Weather Radar Systems, COST 75 International Seminar, Locarno, Switzerland, 23-27 March, 544-556.

Joe, P. and S. Lapczak, 2002: Evolution of the Canadian Operational Radar Network, ERAD Publication Series, 1, 370-382 (2002).

Lapczak, S., E. Aldcroft, M. Stanley-Jones, J. Scott, P. Joe, P. Van Rijn, M. Falla, A. Gagne, P. Ford, K. Reynolds and D. Hudak, 1999: The Canadian National Radar Project, 29th Conf. Radar Met., Montreal, AMS, 327-330.